Predicting Flow Induced Vibration in U-Bend Regions of Heat Exchangers: An Engineering Solution

K.P. Singh
President & CEO
Holtec International
Marlton, NJ

ABSTRACT: *From the standpoint of flow induced vibrations, U-bends of tubular heat exchangers constitute structurally one of the most vulnerable regions. The U-bends possess relatively low out-of-plane frequency enabling them to extract energy from the shell stream at low flow velocities. All published correlations in the literature imply the existence of a direct relationship between the flow velocities and the incidence of large amptitude tube vibrations. Hence it is important to determine the velocity profile in the U-bend region accurately. A method to obtain an engineering solution is proposed herein which may be utilized in conjunction with the available correlations to reliably predict the possibility of vibration. Determination of the flow profile may be further utilized to improve the estimates of shellside heat transfer coefficients.*

I. Introduction

Concomitant with the advent of the nuclear industry, the incidence of detrimental tube vibrations has become a growing concern in heat exchanger design. The genesis of the problem lies in the high unit thermal performance required of the heat exchangers in the nuclear power service. The heat transfering media being generally chemically clean, the fouling factors specified for nuclear heat exchangers are usually quite small (typically in the order of 0.001 sq. ft-Hr.°F/BTU). As a result, the shellside film coefficient has a direct bearing on the overall heat transfer coefficient of the equipment. Thus, the inevitable trend has been towards maximizing the shellside film coefficient, within the available pressure drop, by increasing the shellside flow velocity—thereby sometimes inadvertently introducing tube vibration menace.

One of the most critical regions is the U-bends of U-tube type heat exchangers. Unsupported U-bends generally possess much smaller out-of-plane natural frequency than the straight tube segements (**1**), and hence are more susceptible to flow induced vibrations. Nelms and Segaser (**2**) recommend designing the heat exchangers such that the flow across the U-bends is minimized or even eliminated. In many cases such an expedient is unacceptably expensive, since the U-bends may involve a substantial portion of the total heat transfer surface. Obviously, a much preferable solution is to predict the incidence of vibration of the U-bends, and support those bend midspans which may be threatened by vibration. This article provides the basis for such an approach.

It is now generally recognized that the liquid flow induced vibrations are principally due to two mechanisms, namely vortex shedding (**3–5**), and fluid–elastic feed back (**6, 7**). Although a definitive understanding of the vibration phenomena in tubular heat exchangers is still unavailable, engineering prediction methods in the form of semi-empirical correlations based on the vortex shedding concept have been proposed.

Fitz-Hugh (**8**) describes two such techniques which he calls "resonance" and "severity techniques". The resonance technique assumes that the vortex shedding frequency is directly related to flow velocity through Strouhal number. The Severity technique, due to Thorngren (**12**) proposes damage numbers based on force equilibrium between fluid drag and tube reactive forces. Other correlations due to Owen (**11**), and Connors (**6**) are also used in design practice (**10**).

A key variable in all prediction methods is the cross-flow velocity. A method to estimate the cross-flow velocity in the straight segments has been proposed by Tinker (**9**). Tinker's method has been extensively utilized in determining vibration thresholds as well heat transfer coefficients of straight tube segments. However, no such solution for the U-bend region is reported.

II. Heat Exchanger Configuration

A typical baffle layout is shown in Fig. 1. The inlet nozzle is located beyond the bundle to avoid direct impingement related tube erosion problems. The tubes are arranged in a staggered pattern (usually triangular) on a desired pitch which is determined by available pressure loss, and bundle diameter limitations. The tube pitch to diameter ratio varies in the range of 1.2–1.4. Double segmental baffles, shown in Fig. 1 consist of two basic baffle geometries which

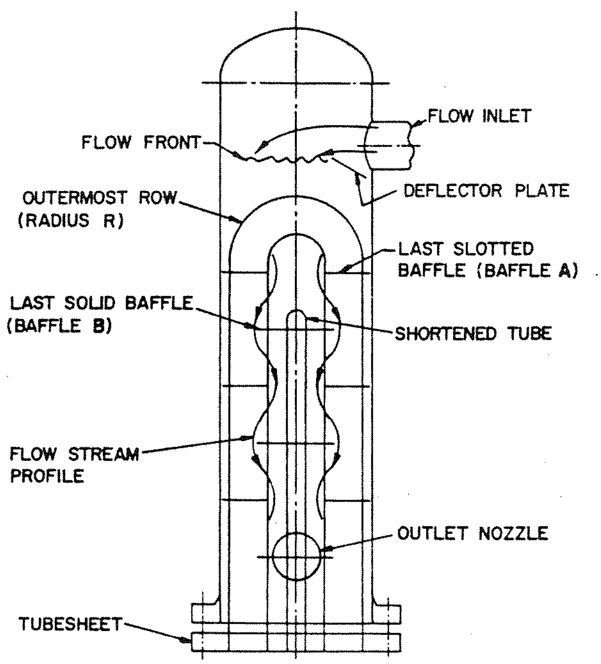

FIG. 1. Typical baffle-tube geometry.

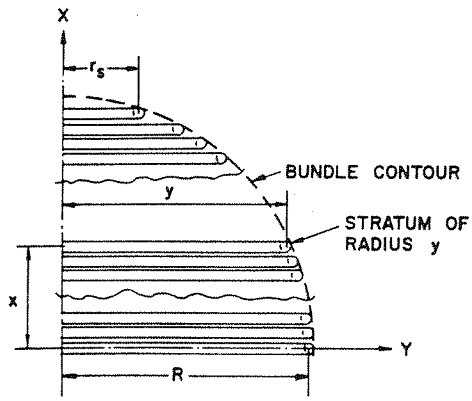

FIG. 2. One-half of U-bundle.

we identify as the "solid baffle" [Fig. 3(b)], and the "slotted baffle" [Fig. 3(a)] respectively. The overlap (in Z-direction) between the two baffles, arranged alternately as shown in Fig. 1, determines the extent of cross-flow of the shellside stream. The last baffle is of the slotted type such that the large diameter U-bends are supported at their points of tangency*. The small diameter U's, not supported by the last slotted baffle, are shortened to reduce their overhang [See Fig. 1]. The so-called shortened tubes thus escape the full thrust of the flow, and can usually be shown to not require any mid-span support. However, the tubes supported by the last baffle "see" the complete shell stream, and hence must be carefully studied and protected from vibration. In the next section, we describe the mathematical model which predicts the flow distribution, and thus enables using the aforementioned correlation techniques to evaluate the vibration potential.

It is worthwhile to point-out that the determination of detailed velocity distribution is an indispensible aid in accurately computing the shellside film coefficient in the U-bend region. Presently, even sophisticated heat exchanger rating computer programs use empirical correction factors to adjust the shellside film coefficients in the U-bend region.

III. Planar Flow Model

A physically admissible flow model in the U-bend region can be constructed by recognizing that the shape of the opening at baffle A and symmetry of the bundle about the y–z plane encourages the flow streams to be parallel to the plane of the U-tubes (y–z plane). The curvature of the shell surface, and orientation of the inlet nozzle may introduce some velocity components perpendicular to the y–z plane, but in general such deviations will be small due to the preponderant geometric symmetry of the bundle. Hence, the flow can be assumed to be essentially stratified parallel to the plane of the U's and flowing radially inwards towards the baffle slit. To the approaching stream, the U-bundle appears to be section of a perforated hemisphere [see Fig. 2]. At height

* In actual practice a small projection of the straight segment beyond the last baffle is provided to facilitate assembly.

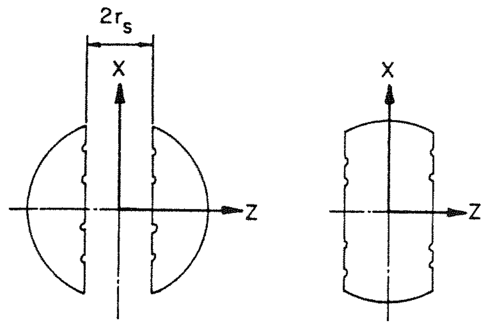

FIG. 3. Double segmental baffle shapes.

x (above the y–z plane), the tube stratum has a maximum radius y. The flow through this stratum of unit width [Fig. 4] is related to the pressure drop ΔP by Eq. (1).

$$\Delta P = \frac{\gamma}{2g}[\psi_1 V_1^2 + \psi_2 \sum_{i=1}^{n} V_i^2] \tag{1}$$

where γ is density of the fluid at its bulk temperature, and g is the gravitational constant. The stratum at height x is assumed to have n tube rows. Let r_i denote the bend radius of ith tube row where the innermost row (radius equal to one half of baffle slot width) is designated as row No. 1. V_i denotes the flow velocity at row i. Thus, the radius of nth row is $r_n = y$, and the associated flow velocity is V_n.

In Eq. (1), the first term in the right hand side represents the pressure loss in contraction and expansion through the baffle window of radius $r_s(=r_1)$ and ψ_1 is the corresponding coefficient. The second term represents the pressure drop as the stream traverses the radial path of length $(y-r_s)$ containing n tube rows. ψ_2 is the corresponding coefficient which lumps the pressure drop due to momentum change, fluid skin friction and turbulence loss in one term. The correlations for ψ_1 and ψ_2 will be further discussed later in this section.

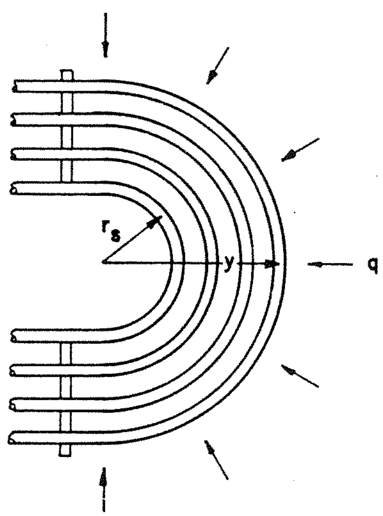

FIG. 4. Radial planar flow at stratum of radius y.

If q denotes the flow rate at this stratum, then mass continuity yields:

$$q = \pi r_i V_i; \quad i = 1, 2, \ldots n. \tag{2}$$

where $r_1 = r_s$.

Substituting for V_1 and V_i from Eq. (2) into Eq. (1), we have

$$\frac{2\Pi^2 g}{\gamma}\frac{\Delta P}{\psi_1} = q^2\left[\frac{1}{r_s^2} + \omega \sum_{i=1}^{n} \frac{1}{r_i^2}\right] \tag{3}$$

where

$$\omega = \frac{\psi_2}{\psi_1}. \tag{4}$$

The numerical sum in Eq. (3) can be replaced by an integral if we note that the trapezoidal rule for numerical quadrature implies that

$$\frac{1}{h}\int_{a_1}^{a_2} f(x)\,\mathrm{d}x = \sum_{i=1}^{n} f_i - 0{\cdot}5(f_1 + f_n) \tag{5}$$

where f_i is the value of function $f(x)$ evaluated at the ith node; and h is the nodal spacing; i.e. $h = (a_2 - a_1)/(n-1)$. Appealing to Identity (5) in Eq. (3) yields:

$$q^2\left[\frac{1}{r_s^2} + \frac{\omega}{p_l}\int_{r_s}^{y}\frac{\mathrm{d}r}{r^2} + \frac{\omega}{2}\left(\frac{1}{r_s^2} + \frac{1}{y^2}\right)\right] = C^2 \tag{6}$$

where

$$C^2 = \frac{2g\pi^2}{\gamma}\frac{\Delta P}{\psi_1} \tag{7}$$

and p_l is the longitudinal pitch, defined as the distance between the tube rows. Thus,

$$p_l = \frac{r_n - r_1}{n-1} = \frac{y - r_s}{n-1}. \tag{8}$$

Performing the necessary integration in Eq. (6), we have

$$q = \frac{C}{\left[\frac{1}{r_s^2} + \frac{\omega}{p_l}\left(\frac{1}{r_s} - \frac{1}{y}\right) + \frac{\omega}{2}\left(\frac{1}{r_s^2} + \frac{1}{y^2}\right)\right]^{1/2}} \tag{9}$$

C is an undetermined constant. The third term in the denominator in Eq. (9) is usually vary small and can be neglected. However, we will retain it in this analysis since it does not appreciably add to the mathematical tedium.

We next note that the flow through the entire bundle surface (segment of a hemisphere), and open baffle window area is given by Q; where

$$Q = A_w V_w + 2\eta \int_0^{x'} q\,\mathrm{d}x \tag{10}$$

where

$$x' = (R^2 - r_s^2)^{1/2}$$

R is the outer bundle radius, η is the perforation coefficient of the bundle surface defined as

$$\eta = \frac{p-d}{p} \tag{11}$$

where p and d are the transverse tube pitch and tube O.D., respectively. A_w is the surface area of a semi-circular cylinder of radius r_s, and length $2(R_s - x')$, where R_s denotes the inside radius of the shell. Substituting for q from Eq. (9) into Eq. (10), and integrating, we have

$$Q = A_w V_w + 2\eta C R^2 I \tag{12}$$

where V_w is the window velocity evaluated at the surface of the semi-circular cylinder of radius r_s.

$$I = \int_0^\rho \left[\chi^2 + \frac{\omega R}{p_l}\{\chi - (1-z^2)^{-1/2}\} + \frac{\omega}{2}\{\chi^2 + (1-z^2)^{-1}\}\right]^{-1/2} dz \tag{13}$$

where

$$z = \frac{x}{R} \tag{14}$$

$$\chi = \frac{R}{r_s} \tag{15}$$

and

$$\rho = (1-\chi^{-2})^{1/2}. \tag{16}$$

If N denotes the number of tube rows at the mid plane of symmetry ($x = 0$), then the expression for I can be recast as follows:

$$I = \int_0^\rho \left[\chi^2 + \frac{\omega\chi(N-1)}{\chi - 1}\{\chi - (1-z^2)^{-1/2}\} + \frac{\omega}{2}\{\chi^2 + (1-z^2)^{-1}\}\right]^{-1/2} dz \tag{17}$$

I is computed for a given ω, χ and N by a suitable numerical quadrature scheme, such as Simpson's rule.

Notice from Eq. (9); at $y = r_s$, $q = q_w$ is given by

$$q_w = \frac{C r_s}{(1+\omega)^{1/2}}. \tag{18}$$

Hence

$$V_w = \frac{C}{\pi(1+\omega)^{1/2}}. \tag{19}$$

Noting that

$$A_w = 2\pi r_s [R_s - (R^2 - r_s^2)^{1/2}]. \tag{20}$$

We have, by combining Eqs. (12), (19) and (20)

$$Q = 2CR^2 \left[\frac{\{\xi - (1-\chi^{-2})^{1/2}\}}{\chi(1+\omega)^{1/2}} + \eta I\right] \tag{21}$$

where

$$\xi=\frac{R_s}{R} \tag{22}$$

ξ is close to 1 for most practical designs. Equation (21) determines C. The velocity profile follows from Eq. (9), which cast in a more direct form below.

$$q=\frac{C}{\left[\frac{1}{r_s^2}+\frac{\omega\chi(N-1)}{(\chi-1)R}\left(\frac{1}{r_s}-\frac{1}{y}\right)+\frac{\omega}{2}\left(\frac{1}{r_s^2}+\frac{1}{y^2}\right)\right]^{1/2}} \tag{23}$$

where q is the volumetric flow rate through a stratum of unit width, and outer radius y. Hence, the velocity $V(y, r)$ at bend radius r in the stratum of outer radius y is given by

$$V(y,r)=\frac{C}{\pi r\left[\frac{1}{r_s^2}+\frac{\omega\chi(N-1)}{(\chi-1)R}\left(\frac{1}{r_s}-\frac{1}{y}\right)+\frac{\omega}{2}\left(\frac{1}{r_s^2}+\frac{1}{y^2}\right)\right]^{1/2}}. \tag{24}$$

Finally, an expression for ω has to be devised. The contraction and expansion coefficient ψ_1 depends on the shape of the orifice, its edge condition, and ratio of contraction and expansion areas. According to Kays (**13**), the contraction coefficient C_c and Expansion Coefficient C_e are given, in the turbulent range*, by

$$C_c=0{\cdot}41(1-\Lambda_1) \tag{25}$$

$$C_e=(1-\Lambda_2)^2 \tag{26}$$

where Λ_1 is the ratio of the area of the contracted stream to that of the uncontracted stream. Similarly, Λ_2 is ratio of the unexpanded stream to the expanded stream cross sectional areas.

A lower bound on C_c and C_e can be obtained by assuming the uncontracted (and expanded) areas to correspond to the surface of the smallest bend. Thus

$$\Lambda_1=\Lambda_2=\frac{2}{\pi}. \tag{27}$$

Furthermore, we note that ψ_1 is referred to the velocity at the semi-cylindrical surface [in Eq. (1)],
hence

$$\psi_1=\frac{\pi^2}{4}(C_c+C_e). \tag{28}$$

From Eqs. (25)–(28), we have

$$\psi_1=0{\cdot}281. \tag{28a}$$

* Contraction and expansion coefficients when multiplied by the velocity head referred to the constricted channel cross section give the corresponding pressure drops.

Equation (28a) will in general give a lower bound for ψ_1, since the expressions for Λ_1 and Λ_2 are obviously overestimates. An upper bound on ψ_1 can be found by setting Λ_1 and Λ_2 equal to the ratio of the baffle cut area A_c to the net longitudinal flow area in the shell A_s. Note

$$A_c = 4R_s r_s \tag{29a}$$

and

$$A_s = \frac{\pi}{4}(4R_s^2 - N'd^2) \tag{29b}$$

where N' is the total number of tubes in the shell adjacent to the baffle. Using the upper bound on ψ_1 in Eq. (1) will overpredict the flow velocities through the bundle. This is discussed further in the following.

Experimentally measured values of the crossflow pressure drop coefficient ψ_2 have been reported by several investigators, notably Bell (**14**). ψ_2 strongly depends on the transverse pitch p, layout arrangement, and to some extent, on the longitudinal pitch. The value of ψ_2 can be found in the literature for the specified bundle geometry as a function of the crossflow Reynolds number, R_e. R_e should be based on the nominal flow velocity V' through the baffle, i.e.

$$V' = \frac{Q}{A_c}. \tag{30}$$

Unfortunately, accurate values of ψ_1 and ψ_2 are not known at present. Parametric experimental studies on prototypes is required to develop precise correlations for ψ_1 and ψ_2. It is recommended to use the upper bound on ψ_1 as developed in the foregoing. Furthermore, since ψ_2 is based on a higher Reynolds number than is actually present in most of the bundle, the value of ψ_2 calculated will be a lower bound. Hence, the dimensionless ratio ω will also be a lower bound. In physical terms, this implies that the flow path resistance of the bundle is underestimated and that of the frontal window region A_w is overestimated. Consequently, the flow velocities through the bundle will be overpredicted. From the view point of predicting flow induced vibration, the direction of error in the velocity magnitudes is favorable. However, the error in calculating the shell side film coefficient will be on the unsafe side. Numerical studies indicate that the maximum increase in the flow velocity in typical tube bundles is less than 10% when ω is decreased by a factor of 4. Thus, a precise knowledge of ω does not appear to be crucial to the accuracy in prediction of the velocity field.

Finally, for the sake of comparison we will compute the nominal flow velocity V^* penetrating the bundle surface, assuming that the flow was uniform over the surface and the frontal window area A_w. It follows that

$$Q = 2\pi\eta V^* \int_0^{x'} y\, dx + A_w V^* \tag{31}$$

or

$$Q = V^*[2\pi\eta(0{\cdot}5\, R^2)\{\alpha + 0{\cdot}5 \sin 2\alpha\} + 2\pi r_s\{R_s - (R^2 - r_s^2)^{1/2}\}] \tag{32}$$

where

$$\alpha = \sin^{-1} \rho \tag{33}$$

or

$$Q = 2\pi R^2 V^*[0{\cdot}5\eta\{\alpha + 0{\cdot}5 \sin 2\alpha\} + \frac{1}{\chi}\{\xi - (1-\chi^{-2})^{1/2}\}]. \tag{34}$$

Equation (34) determines V^*.

IV. Example

To illustrate the method, the results for a two tube pass, U-tube heat exchanger of 24·75 in. inside dia. is given. The maximum bend radius R is 11·8 in., and the baffle slit radius r_s is 3·69 in. The perforation efficiency η is 0·2(0·75 in. O.D. tubes laid out on 0·9375 in. pitch). There are a total of 11 tube rows in the midplane of the bundle ($x = 0$). The volumetric flow rate Q is 21732 in.^{3}/sec.

The velocity distribution corresponding to $\omega = 1$ for $y^* = y/R = 0{\cdot}381$, 0·588, 0·794, and 1 is plotted in Fig. 5 as a function of tube radius $r^* = r/R$. Some important general inferences may be drawn from Fig. 5. The velocity decreases monotonically with increasing y for a given tube radius. The velocity at the maximum bend radius ($x = 0$) may be a small fraction of the velocity in the baffle window, V_w. In the example problem, the ratio of the velocity at the maximum bend radius to the maximum window velocity V_w is found to be 0·204. Thus, for U-bundles with wide pass partition gaps near the largest bend radii, the window effect may produce localized high velocities. In such instances, the openings should be either closed using dummy tubes, or the midspans of such tubes should be adequately supported.

The fundamental natural frequency, f_n, of the tube bend of largest radius, $R = 11.8$ in. was calculated to be 36 cps (U-bends with 0·88 in. straight overhang). Using the Resonance technique, the dimensionless number S characterizing vortex shedding frequency f is 0·4 (estimated from Fig. 3 of Ref. (**8**).

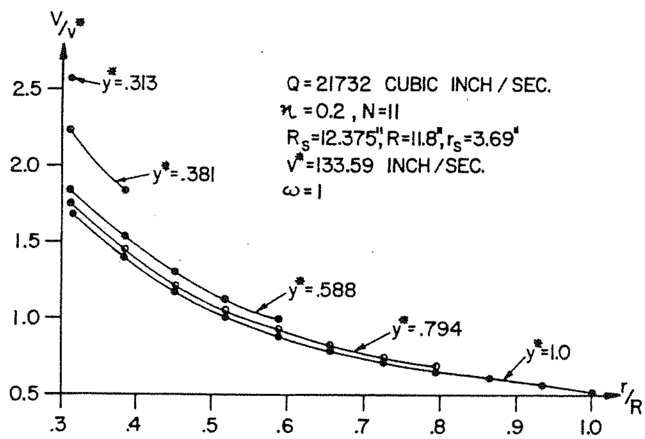

FIG 5 ; VELOCITY PROFILE FOR TYPICAL TUBE LAYERS (EXAMPLE PROBLEM)

In terms of S, the vortex shedding frequency is given by

$$f = \frac{SV}{d} \tag{35}$$

where V is the corresponding flow velocity, and d is outside tube diameter. The flow velocity at $R = 11{\cdot}8$ in. is found to be 70·1 in./sec. Hence Eq. (35) yields $f = 37{\cdot}4$ cps. Notice f exceeds f_n, and hence the possibility of damaging tube vibrations and "lock-in" phenomenon exists. This calculation may be made for every tube row. Since the cross-flow velocity varies in a given tube row as a function of y, the tube with the maximum cross-flow velocity in each row should be examained. In this manner, the tube rows requiring intermediate bend supports can be identified.

V. Conclusion

A method to predict the flow distribution in the U-bend region of tubular heat exchangers has been developed. The solution procedure assumes the tube layout of a uniform pitch, and a slotted baffle support at the point of tangency of the U-bundle. It is shown, via a numerical example, that the flow velocity exhibits a strong dependence on tube radius, and location of the tube in the tube row (tube stratum). The prescription proposed herein can be used to predict the onset of flow induced vibration and to accurately evaluate the shellside film coefficient. To the best of our knowledge, this is the first mathematical solution of the title problem in the open literature.

Acknowledgement

The author is thankful to Mr. Michael J. Holtz for his help with the numerical computations.

References

(1) L. S. S. Lee, "Natural frequency of heat exchanger tubes", *Symp. Appl. of Solid Mech.*, University of Waterloo, Canada, June 26–27, 1972.

(2) H. A. Nelms and C. L. Segaser, "Survey of nuclear reactor system primary circuit heat exchangers, Oak Ridge National Lab. Rep. No. ORNL-4399, April, 1969.

(3) Y. N. Chen, "Flow induced vibration and noise in tube-bank heat exchangers due to von Karman streets", *Trans. ASME Ser. B. J. Engng. for Industry*, Vol. 90, pp. 134–146, Feb., 1968.

(4) R. E. D. Bishop and A. Y. Hassan, "The lift and drag forces on a circular cylinder in a flowing fluid", *Proc. Royal Soc., Lond. Ser. A*, Vol. 277, pp. 32–50, 1964.

(5) O. M. Griffin, "Flow near self-excited and forced vibrating circular cylinders", *Trans. ASME, Ser. B*, Vol. 94, *J. Engng. for Industry*, pp. 539–547, 1972.

(6) H. J. Connors, "Fluide–elastic vibration of tube arrays excited by cross flow", *Symp. on Flow Induced Vibration in Heat Exchangers*, pp. 42–56, ASME Annual Winter Mtg., New York, 1970.

(7) R. D. Blevins, "Fluid–elastic whirling of a tube row", *Trans. ASME J. Pressure Vessel Tech., Ser. J*, Vol. 96, pp. 263–267, Nov. 1974.

(8) J. H. Fitz-Hugh, "Flow induced vibration in heat exchangers", *Int. Symp. on Vibration Problems in Industry*, Keswick, U.K., April 10–12, 1973.

(9) T. Tinker, "Shellside characteristics of shell-and tube heat exchangers: A simplified rating system for commercial heat exchangers", *Trans. ASME*, Vol. 80, pp. 36–52, Jan. 1958.

(10) J. M. Chenoweth and R. S. Kistler, "Tube vibrations in shell and tube heat exchangers", *AICHE–ASME 15th Natl. Heat Transfer Conf.*, San Francisco, Calif., Aug. 10–13, 1975.

(11) P. R. Owen, "Buffeting excitation of boiler tube vibration", *J. Mech. Engng. Sci.*, Vol. 7, pp. 431–439, 1965.

(12) J. T. Thorngren, "Predict exchanger tube damage", *Hydrocarbon Processing*, pp. 129–131, April, 1970.

(13) W. M. Kays, "Loss coefficients for abrupt changes in flow cross-sections with low Reynolds number flow in single and multiple tube systems", *Trans. ASME*, Vol. 72, pp. 1067–1074, 1950.

(14) K. J. Bell, "Final report of the cooperative research program on shell and tube heat exchangers", Bull. No. 5, Univ. of Delaware Eng. Experiment Station, 1963.